



REVIEW

An overview of de novo bone generation in animal models

Takashi Taguchi  | Mandi J. Lopez 

Laboratory for Equine and Comparative Orthopedic Research, Department of Veterinary Clinical Sciences, School of Veterinary Medicine, Louisiana State University, Baton Rouge, Louisiana, USA

Correspondence

Mandi J. Lopez, 1909 Skip Bertman Dr., Baton Rouge, LA.
Email: mlopez@lsu.edu

Funding information

Tynewald Foundation; Louisiana State University Equine Health Studies Program

Scientific editing by Clare Yellowley.

Abstract

Some of the earliest success in de novo tissue generation was in bone tissue, and advances, facilitated by the use of endogenous and exogenous progenitor cells, continue unabated. The concept of one health promotes shared discoveries among medical disciplines to overcome health challenges that afflict numerous species. Carefully selected animal models are vital to development and translation of targeted therapies that improve the health and well-being of humans and animals alike. While inherent differences among species limit direct translation of scientific knowledge between them, rapid progress in ex vivo and in vivo de novo tissue generation is propelling revolutionary innovation to reality among all musculoskeletal specialties. This review contains a comparison of bone deposition among species and descriptions of animal models of bone restoration designed to replicate a multitude of bone injuries and pathology, including impaired osteogenic capacity.

KEYWORDS

animal models, bone regeneration, critical size bone defects

1 | INTRODUCTION

The goal and focus of innumerable scientific efforts throughout recorded history was to decipher and harness the power and unlimited potential of the cell. Discovery, isolation, and culture of cells that can assume characteristics of numerous lineages, including those from distinct embryonic layers, ignited a virtual explosion of discovery in the vast arena of cell therapies over the last two to three decades. A natural trajectory of the therapeutic momentum is to replace musculoskeletal tissue compromised by trauma, disease, or malformation with healthy tissue via de novo tissue generation. Broad approaches include in vitro generation of viable, implantable tissue, and application of exogenous cells and materials to recruit and direct endogenous cells. Carriers for cell delivery are composed of materials that facilitate tissue formation by progenitor cells, and they are routinely customized at the macro-, micro-, and ultra-structural levels to replicate tissue matrix, including organic

and inorganic components. Tremendous advances in de novo tissue generation provide unlimited opportunities to restore musculoskeletal tissue and impact the health and wellbeing of global community members at any stage of life.

The process of moving innovative de novo musculoskeletal tissue generation from concept to clinical reality is incremental and iterative. Key elements of successful translation from bench to bedside are reproducible animal models that recapitulate targeted musculoskeletal pathology. Models vary widely among joints and limbs and between traumatic, degenerative, and developmental conditions. Many are induced by surgical or chemical means, and test therapies are applied immediately or after a period of time following the initial injury. Numerous considerations are associated with selection of an animal model. There are specific factors related to the scientific questions or techniques to be tested and practical considerations like animal cost, availability, and regulation-compliant surgical and housing facilities.

This is an open access article under the terms of the Creative Commons Attribution-NonCommercial-NoDerivs License, which permits use and distribution in any medium, provided the original work is properly cited, the use is non-commercial and no modifications or adaptations are made.

© 2020 The Authors. *Journal of Orthopaedic Research*® published by Wiley Periodicals LLC on behalf of Orthopaedic Research Society

TABLE 1 Animal model long bone characteristics

	Small mammal	Large mammal	NHP and human
Sexual maturity age	Murine: 6–8 weeks ⁷ Rat: 6 weeks ¹⁰ Lapin: 10–12 weeks ¹³	Canine: 7–21 months ⁸ Ovine: 7–8 months ¹¹ Porcine: 5–6 months ¹¹ Equine: 7–14 months ¹⁰	Human: ~17 years ⁹ NHP: 4–6 years ¹²
Skeletal maturity age (Growth plate closure age/life expectancy age x 100) ¹⁴	Murine: 16–24 weeks (13.9–27.8) ⁷ Rat: 24–32 weeks (22–35) ¹⁰ Lapin: 28–30 weeks (5.5–8.1) ¹³	Canine: 10–11 months (4.3–6.9) ⁸ Ovine: ~40 months (9.4) ¹⁶ Porcine: 18–22 months ^{11,19,20} Bovine: 12–37 months (6.7–20.1) ¹⁴ Equine: ~3 years (5.8–6.3) ²¹	Human: ~25 years (16.7–25) ¹⁵ NHP: 7.2–10 years (11.2–17.5) ^{17,18}
Fractional area of secondary bone (FASB)	Rat: minimal ²² Lapin: minimal ²⁵	Ovine: 2%–91% ²³ Bovine: ~11% ²⁴ Equine: 5%–75% ^{23,27}	Human: ~48% ²⁴ NHP: 61%–74% ²⁶
Bone remodeling period	Murine: ~2 weeks ⁷ Rat: ~6 days ³⁰ Lapin: 70 days ³³	Canine: ~2 months ^{28,29} Ovine: ~80 days ³¹ Porcine: 1–5 months ³²	Human: 6–9 months ⁷ NHP: 8–24 months ³²
Bone formation rate/ bone volume (BFR/ BV) at skeletal maturity (bone type)	Murine ^a : ~1900% (cancellous) ^{34–36} Rat: ~19% (cortical) ⁴² ~1158% (cancellous) ⁴⁴ Lapin: ~20.7% (cortical) ³³	Canine: 0.5%–6.4% (cortical) ^{28,37,38} 20%–50% (cancellous) ³⁸ Ovine: 55%–72% (cancellous) ⁴⁵ Porcine: ~53% (cancellous) ³² Equine: ~10% (cortical) ⁴⁸	Human: 3%–4% (cortical) ^{39–41} ~26.3% (cancellous) ⁴³ NHP: 13%–38% (cancellous) ^{46,47}
Pelvic limb axial force	Lapin: 201% BW ⁴⁹	Caprine: ~100% BW ^{50,51} Ovine: 48% BW ⁵³	Human: 470% BW ⁵²

Abbreviations: BW, body weight; NHP, nonhuman primate.

^akeletally immature.

Published substantiation of, and investigator experience with a model in addition to validated outcome assessment assays, including proteomic and genomic panels, also guide selection. Customized genetic makeup and immunodeficiency are found primarily in rodents. Findings from such highly tailored models require testing in larger mammal models before clinical translation and implementation.

Orthotopic evaluation of bone healing in a large animal model is frequently part of the final preclinical testing stages. In addition to anatomy and magnitude of load bearing,¹ bone formation and microstructure are critical assessments of an animal model (Table 1). It is also important to remember that, while bone composition is relatively highly conserved, it is not identical among species²; canine and porcine are relatively close in composition and density to human, while rat has few similarities. Additionally, bone regeneration declines and morphology³

changes differently with age among distinct life spans.^{4,5} This is especially relevant to defining critical size defect (CSD)⁶ sizes at various maturity levels in animals (Table 2). The following sections provide an overview of animal bone regeneration models beginning with a general comparison of bone turnover rates.

2 | BONE FORMATION DURING NORMAL HOMEOSTASIS

2.1 | Bone remodeling

For comparisons among species, the rate of natural bone formation during normal homeostasis should be considered (Table 1, Figure 1).

TABLE 2 Critical defect size and fixation among bones and species

Bone	Species	Defect size (mm)	Fixation	Potential advantages
Calvarium	Murine	>Ø 2 ^{54,55}		
	Rat	>Ø 5 ^{56,57}		
	Guinea Pig	10 ⁵⁸		
	Lapin	>Ø 6 ^{59,60}		
	Canine	20 ^{61,62}		
	Ovine	>30 ⁶³⁻⁶⁵		
	Porcine	>Ø 10 ^{66,67}		Bone composition similar to human ²
Rib	Canine	>50 ^{68,69}		Thoracic wall kinetics similar to human ^{70,71}
	Ovine	40 ⁷²	Plate	
	Porcine	100 ⁷³		
Ilium	Lapin	>Ø 5 ^{74,75}		
	Caprine	>Ø 8 ⁷⁶⁻⁷⁸		
Humerus	Lapin	>7 ⁷⁹⁻⁸¹	Plate, intramedullary rod	
	Canine	>Ø 5 ⁸²⁻⁸⁶		
	Ovine	>Ø 6 ⁸⁷⁻⁸⁹		
Radius	Rat	>5 ^{90,91}		Segmental defect without fixation possible Established radiographic and histologic scoring system ⁹⁵
	Lapin	>14 ⁹²⁻⁹⁴		
		>10 ⁹⁶⁻⁹⁸	Plate	
Femur	Rat	>4 ⁹⁹⁻¹⁰³	Plate, external fixator, Intramedullary rod	Highly standardized fixation systems Macrostructurally similar to human ¹ Macrostructurally similar to human ¹ Bone composition similar to human ²
	Canine	>21 ¹⁰⁴⁻¹⁰⁷	Plate, Intramedullary Rod	
	Caprine	Ø 8 ⁷⁶		
Tibia	Lapin	15 ¹⁰⁸	Plate	Defect strain similar to human
	Ovine	>30 ^{4,109-112}	Plate, external fixator	
Vertebrae	Rat	>Ø 3 ¹¹³⁻¹¹⁵		
	Caprine	Ø 5 ⁷⁶		
	Ovine	>Ø 6 ¹¹⁶⁻¹²²		
Mandible	Rat	>Ø 3 ¹²³⁻¹²⁸		Macrostructure and microstructure and masticatory force similar to human ^{132,133}
	Porcine	>17 ¹²⁹⁻¹³¹		

Note: Ø, cortical defect diameter.

Two measures of bone activity are the extent of remodeling and rate of remodeling. Both vary with species, age, bone, and bone region. The fractional area of secondary bone (FASB), area comprised of secondary osteons in cortical bone, represents the amount of remodeling present. It is defined as the percentage of the total area of secondary bone relative to the total area of interstitial bone and secondary bone together.¹³⁴ The higher the FASB, the greater the extent of bone remodeling. In general, the amount of remodeled bone increases with age. Additionally, bone regions under compressive stress have the highest extent of remodeling and therefore secondary osteons while those under tensile stress retain more primary bone.^{23,135-137} Due to anatomical differences among species, there are regional differences within bones. As an example, the human femur experiences largely compressive stresses,^{138,139} while most quadruped femurs are subjected to both tensile and compressive stress;

this leads to important species-specific characteristics in regional bone remodeling.¹⁴⁰

Bone maturity is an important consideration in animal models. Broadly speaking, humans and nonhuman primates have highly remodeled cortical bone at maturity followed by large mammals; small mammals like lapin, rat, and murine have minimal remodeled bone as adults.^{24-26,141} Among large mammals, the canine and equine FASB are closest to that of human.^{23,27,142,143} Another distinct difference between animal and human bone is the prominent proportion of plexiform bone, a form of primary bone present during bone growth in rapidly growing mammals, that can result in a relatively low FASB (Figure 2).^{23,24,144} Large mammals typically develop secondary bone near the endosteum while plexiform bone remains adjacent to the periosteum.²² Additionally, the relative size of the osteonal resorption and Haversian

canal areas within secondary osteons is positively correlated with body mass; the higher the body mass, the greater the area of each. Animals close in size to human counterparts may have similar secondary osteon structures.¹⁴⁵

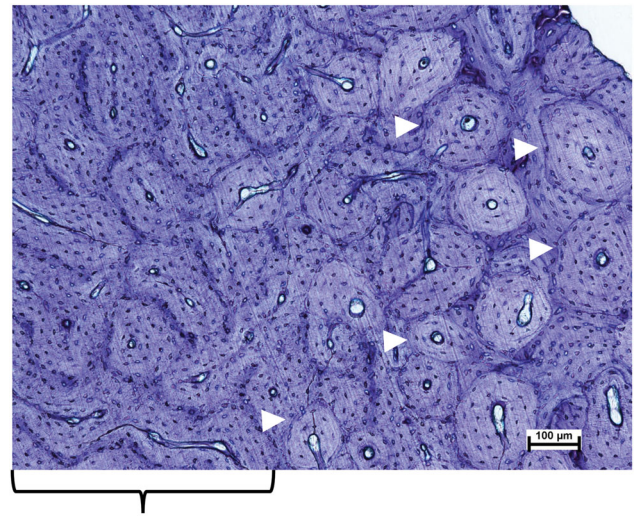
2.2 | Bone formation rate

Distinct from the amount of remodeled bone is the rate of trabecular or cortical bone turnover, often measured as the bone formation rate per unit of bone volume (BFR/BV).¹⁴⁶ In humans, the BFR/BV is a well established measure^{147,148} that is affected by age,¹⁴⁹ use,^{42,150} and comorbidities.^{39,151,152} In animal models, it is used to assess both the rate of bone remodeling and bone healing.¹⁵³ In general, BFR/BV is higher in cancellous bone than cortical bone, and tends to be higher in small versus large mammals and lowest in human cortical and cancellous bone.^{28,32-48} Age has a large impact on BFR/BV in animal models. In rats, the BFR/BV of the proximal tibial metaphysis varies from 290.9% and 335.2% at 1 and 3 months of age, to 61.9% and 80.1% at 6 and 14 months of age, respectively¹⁵⁴; in dogs, the BFR/BV of the femoral mid-diaphysis is 72% in immature and 1%–6.4% in mature animals.^{28,37} The process of bone remodeling during normal homeostasis is somewhat demonstrative of, but not identical to, bone healing capacity.¹⁵⁵ Additionally, the FASB and BFR/BV permit some relative comparisons among species, but they are only two representative measures of normal bone remodeling (Figure 1). Any number of measures may be used or combined to monitor inherent bone forming capability,¹⁴⁶ an important consideration when utilizing animal models to test bone regeneration strategies.

3 | MODELS OF BONE REGENERATION

3.1 | Flat Bone

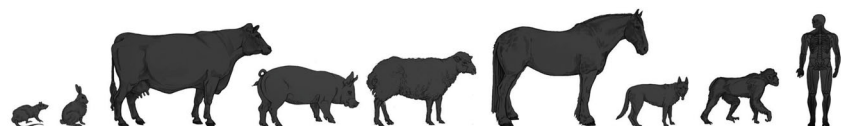
Common flat bone models include the calvarium, costae, and ilium. These non-load bearing bones permit use of multiple CSDs without fixation, and intramembranous ossification is highly conserved among species.^{156,157} Among the three, full-thickness (bicortical), round defects in the rodent



Plexiform Cortical Bone

FIGURE 2 Photomicrograph of an undecalcified section of ovine endosteal cortical bone from the radius. Plexiform cortical bone is on the left. Active remodeling is indicated by the presence of secondary osteons (white arrow heads) on the right. Toluidine blue stain. Scale bar = 100 μ m. (Photo courtesy of Dr. Clifford Les) [Color figure can be viewed at wileyonlinelibrary.com]

and lapin calvarium are the most popular for initial in vivo, orthotopic, and non-orthotopic testing (Figure 3).^{56,57,59,60} Notably, the dura mater is reported to be a source of bone morphogenetic protein 2 (BMP-2) in young animals that seems to diminish with age.^{58,158} The surgical procedure for calvarial defect creation is relatively simple, and the thin murine calvarium permits in vivo cell imaging with multi-photon microscopy to investigate spatiotemporal coordination of cells that contribute to bone healing.¹⁵⁹ As an example, two-photon microscopic imaging was used to confirm that exogenous bone marrow derived multipotent stromal cells on collagen/hydroxyapatite scaffolds were primarily responsible for new bone formation in murine calvarial defects while host cells participated most in periosteum regeneration.¹⁶⁰ Both circular defects and craniectomies are reported in large mammals like canine, ovine, and porcine in which osteotomies recapitulate craniectomies for



Remodeled Cortical Bone

FIGURE 1 Animal and human remodeled cortical bone (fractional area of secondary bone) and bone formation rate (bone formation rate per unit of bone volume) with wedge area representing relative amounts and rates [Color figure can be viewed at wileyonlinelibrary.com]



congenital malformation, trauma, and neoplasia.^{61-64,161} Instrumented transport osteogenesis models are reported as well as self-retaining materials that facilitate detailed magnetic resonance imaging.⁶¹⁻⁶⁴ Collectively, calvarial defect models in both small and large mammals are valuable models for proof-of-concept testing in non-load bearing bone.

Costal bone is a common harvest site for autologous bone and costochondral grafts, and thoracic surgery or trauma can necessitate rib resection.¹⁶²⁻¹⁶⁴ Rib ostectomy models to test rib regeneration options are designed to address pain, instability, and cosmesis associated with large defects.^{72,73,165,166} In part, due similarity in size to human, ovine models of rib resection are common.^{72,167,168} Thoracic wall reconstruction models are typically in species that share human thoracic cavity dynamics like canine and lapin.^{68-71,169} A concavoconvex costovertebral joint¹⁷⁰ in cursory mammals like humans facilitates thoracic cavity expansion by intercostal and diaphragmatic musculature.^{171,172} Non-cursory mammals like caprine and ovine species have a flat costovertebral joint that relies on diaphragmatic musculature for thoracic expansion.¹⁷⁰

The iliac crest is another non-load bearing bone used for materials testing with the important distinction of healing by

enchondral ossification. Caprine and ovine models of circular unicortical or bicortical defects along the iliac crest are popular because microstructural cancellous bone volume and connectivity are similar to human^{173,174} and ovine models of osteoporosis are well established.^{175,176} The ilium is one of the most common sites of autologous cancellous and corticocancellous bone graft harvest.^{163,177} Vascularized iliac bone block resections for treatment of avascular bone lesions or multiple corticocancellous bone harvests for staged surgical reconstructions drive efforts to enhance iliac bone regeneration.¹⁷⁸⁻¹⁸⁰ For large defects and iliac bone blocks, the ovine is particularly advantageous due to anatomical properties that are close to that of human.¹⁸¹ The ovine ilium has only a slightly longer iliac shaft and smaller wing than the human female.

3.2 | Long Bone

Many animal models of long bone generation correspond to the most prevalent long bone fractures in humans.^{76,92,182-184} Multiple, round, unicortical or bicortical, CSDs and non CSDs are used for orthotopic

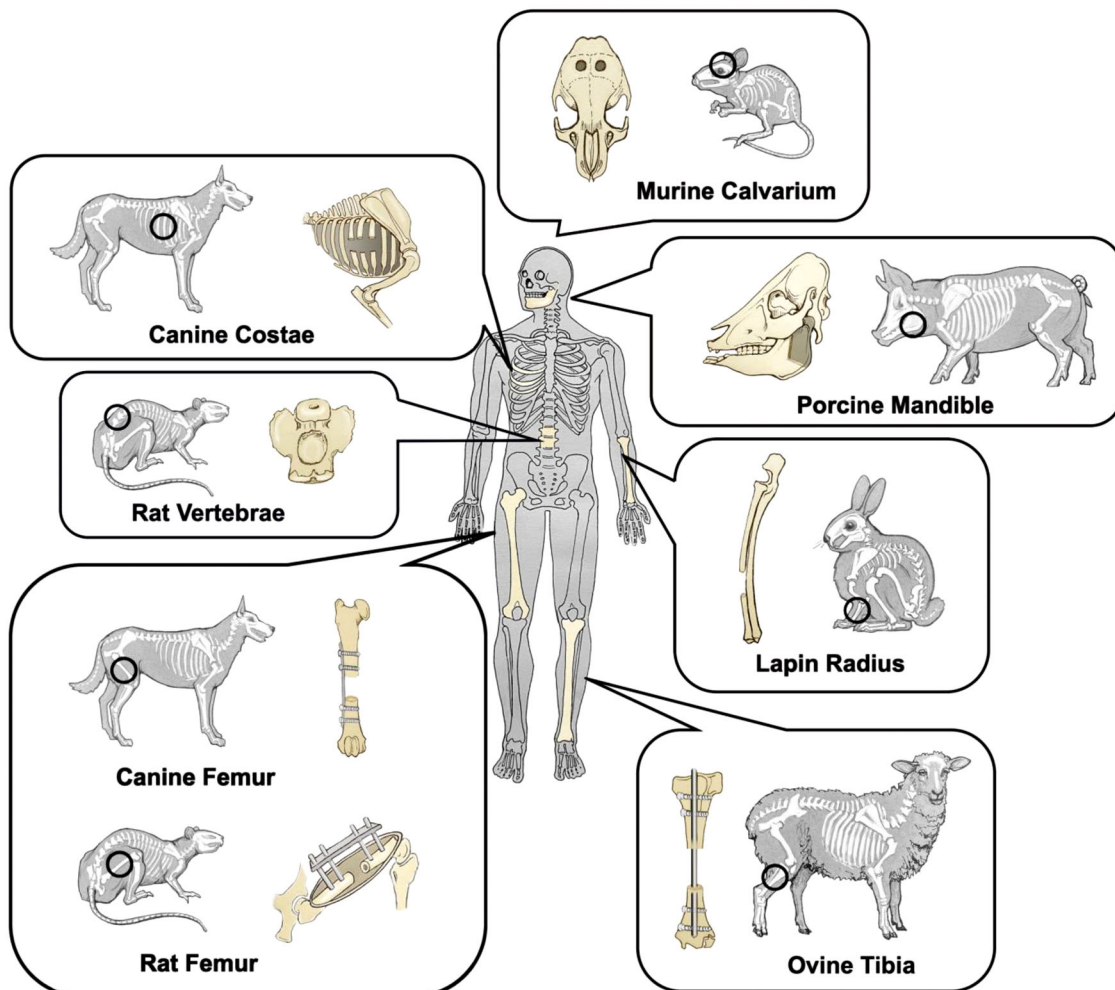


FIGURE 3 Schematic representation of common animal bone defect models [Color figure can be viewed at wileyonlinelibrary.com]

testing in virtually every bone of large and small animals.^{87,185} Defect creation typically requires minimal soft tissue trauma and internal fixation is not required. Models that incorporate ostectomy or osteotomy require internal or external stabilization.^{58,186-190} Large animal models have advantages of large defects and use of standard surgical tools and devices that are not possible in small animals.¹⁹¹ As a general rule, long bone diaphyseal CSDs correspond to approximately 2–2.5 times the diaphyseal diameter, about 3–5 cm in ovine^{109,192-194} or 3 cm in porcine¹⁹⁵ adult tibiae. Osteotomies are typically used to represent comminuted or unstable fractures while osteotomies represent minimally displaced fractures with limited comminution.¹⁹⁶

As indicated above, load bearing varies between quadrupeds and bipeds, especially in the forelimb equivalent of human arms. Based on bone mineral density changes in astronauts, bone deposition in the human pelvic limb is especially responsive to frequency and magnitude of loading, while the thoracic limb is less so.^{135,197-201} The relative physiologic load is comparably higher in the forelimbs and lower in the hind limbs of most animal models. Large mammals bear about 60% of body weight on the forelimbs while rodents and lapin bear approximately 55%.^{202,203} In terms of tibial loading at a walk, the lapin⁴⁹ is reportedly closest to human,⁵² 201% and 470% of body weight, respectively, while caprine is about 100% of body weight.⁵⁰ These important distinctions must be carefully considered when selecting animal models and comparing results among species. Specific information about popular long bone models is provided below (Figure 3).

3.2.1 | Thoracic Limb

There are a number of animal models to assess proximal humeral epiphyseal and metaphyseal bone regeneration.^{82-84,87-89,204} In part due to anatomical congruity between the human and canine humerus, canine cylindrical defect models are commonly employed in young to aged adult dogs.^{82-85,204} Additionally, proximal humeral osteosarcoma occurs naturally in adolescent to young adult dogs, 18–24 months, somewhat analogous to human adolescents.²⁰⁵ These points support the value of canine models to optimize osteogenesis in the proximal humerus. A typical critical size cylindrical defect in the canine proximal humerus is about 5 mm wide and 4 mm deep in middle-size dogs (25–35 kg).²⁰⁶ A valuable stage to assess treatment effects in the model is reportedly during the fibrous to lamellar bone transition between 4 and 6 weeks postoperatively.^{82,84-86} In addition to histologic and histomorphometric analyses, electron probe microanalysis can be used to determine regenerated bone maturity based on chemical composition, typically the calcium/phosphorus ratio.^{82-85,204,207} Using the outcomes above and a proximal metaphyseal cylindrical defect model in young (1–2 years) and senior (10–12 years) adult dogs, transforming growth factor- β 2 on titanium cylinders increased bone volume to tissue volume by three-fold compared with implant alone, though regenerated trabeculae were thinner and unmineralized osteoid higher in senior animals.⁸⁴

A popular segmental defect model in the humerus is in the lapin mid-diaphysis.⁷⁹⁻⁸¹ CSDs in skeletally mature rabbits are around 7 mm long and stabilized with an intramedullary rod or bicortical plates.⁷⁹⁻⁸¹ In vivo monitoring is typically via radiography and nuclear scintigraphy, and postmortem histology is standard.⁷⁹⁻⁸¹ Determination of torsional strength and stiffness via mechanical testing is well established and consistent with predominant physiologic stresses.^{81,208,209} Complete healing of segmental defects can be achieved as early as 6 weeks, but there is a high rate of non-union up to 8 months after injury, 43%–100%, reportedly a result of poor healing capacity.⁷⁹⁻⁸¹ This makes the model appealing for developing treatments to overcome similar complications in human humeral fractures.²¹⁰⁻²¹² In one report, titanium mesh implants with BMP-2 in polymer gel had 100% complete bony bridging of 15 mm humeral defects 6 weeks after implantation, while none of the defects without implants achieved bridging.⁸⁰ This and other reports help establish that the lapin humeral segmental defect model is amenable to testing therapies for suboptimal healing capacity.^{79,81}

Most lapin and rat species have a radio-ulnar synostosis.^{90-94,96,97} Though load bearing is shared between the bones, radial osteotomies are stable and do not require internal fixation.^{90,91,93,94} At lapin skeletal maturity, segmental radial defects range from 10 to 14 mm, though 14 mm is recommended for a CSD; the segmental radial CSD in a skeletally mature rat is greater than 5 mm.^{90,91,93,94,96,97} Radiography and microcomputed tomography (μ -CT) as well as histology outcome measures are standard,^{90,91,93,94} and the Lane–Sandhu scoring system for both radiograph and histologic quantification of bone healing⁹⁵ facilitates comparisons among studies.^{90,91,94} Serum biomarkers are also possible outcome measures; prolonged healing in aged rats is associated with significantly lower levels of bone biomarkers like osteocalcin and alkaline phosphatase.²¹³ Evidence of rat and lapin radiographic bony bridging typically coincides with full recovery of mechanical strength in compression and bending.^{90,91,96} Nanoindentation of thin sections ($\sim 100\ \mu\text{m}$) to measure modulus and hardness of new bone has also been reported in the lapin model.⁹⁸ Although less common, segmental radial osteotomies are reported in Yucatan miniature swine which also have a radio-ulnar synostosis.²¹⁴ Previously, 25–30 mm long defects filled with polymeric membrane in one-year-old animals were bridged radiographically by 8 weeks.²¹⁴ The miniature swine model has unique advantages of a large size without the need for internal or external fixation.

3.2.2 | Pelvic Limb

The most common femoral segmental defect models are rat and murine. Anatomically, the rat femur resembles that of human, and femoral neck and greater trochanter ossification centers do not coalesce in either species. Closure of the rat and murine femoral and tibial physes relative to lifespan are comparable to humans and later than other mammals.¹⁴ Immunocompromised rodent strains permit testing of xenogeneic cells and biomaterials. Recently, human adipose stromal vascular fraction cells on ceramic scaffolds that

enhanced bone formation in immunocompromised rats in preclinical testing also promoted proximal femoral fracture healing in a clinical trial.⁹⁹ Detection of human cells in immunocompromised animals can be accomplished by standard methods including identification of human genetic sequences and antigens by *in situ* hybridization and immunolabeling, respectively.⁹⁹ Commercially available fixation systems for rodent femoral stabilization range from radiolucent plates⁹⁹ and interlocking nails¹⁰⁰ to external fixators.^{99,101} Segmental defects greater than 4 mm in adult rats require about 8 weeks for complete bridging, though study end points typically range from 4 to 12 weeks, and bone formation is monitored similarly to the rodent forelimb.⁹⁹⁻¹⁰² Evaluation of bone mineral density in regenerated rat bone with scanning electron microscope-based quantitative back-scattered electron imaging has been reported.^{101,215} Mechanical tests are frequently designed to assess torsional properties, though mechanical testing varies widely.^{99,103} A potential disadvantage of the rodent femoral defect model is the well-recognized robust healing capacity with and without fixation that can necessitate outcome validation in larger mammals.²¹⁶

Similarities between human and canine femoral anatomy contribute to the value of the canine femoral segmental defect model despite thinner cortices in the canine bone.^{1,217,218} Intramedullary rods or cortical plates are used to stabilize CSDs of at least 21 mm in skeletally mature, middle- to large-size dogs (12–55 kg).¹⁰⁴⁻¹⁰⁷ Outcome assessments are similar to other species, bony bridging typically occurs around 12 weeks, and remodeling has been monitored for extended periods, 24 weeks or more, postoperatively.¹⁰⁴⁻¹⁰⁷ Unlike small mammals, however, recovery of mechanical strength does not always coincide with radiographic healing; this is likely a consequence of extensive remodeling associated with canine bone healing, similar to human bone.^{107,219} Use of gait kinetics to quantify limb use are fairly common in canine studies.^{220,221} Ground reaction forces measured with a force platform are positively correlated with bone healing and have a strong association with callus mineralization and defect stiffness.²²² A recent study showed that addition of human osteogenic protein-1 to cortical allograft strips in canine femoral defects improved limb use over allograft alone 10 weeks after surgery.¹⁰⁴ Wide use of canine gait kinetic measures permits comparisons among a multitude of orthopedic studies, including those with a focus on accelerated bone formation.^{220,221}

Among long bones, tibial osteotomies are frequently used to model traumatic bone loss.²²³ As mentioned above, lapin tibial loading is closer to human than other small mammals, so the lapin tibial mid-diaphyseal segmental defect model, typically stabilized with a bone plate, may have the strongest translational value.^{49,52,53,108} In a large animal model, ovine tibial defects of 30 mm or more in the mid-diaphysis are often treated with plates or external fixators and monitored by standard means up to 3 to 12 months followed by histology and mechanical testing.^{4,109-112,224} The ovine tibial diaphysis has a relatively simple cylindrical macrostructure and loading mechanism compared to more structurally complex bones.²²⁵⁻²²⁷ This, in addition to similarity in weight to adult humans, lends itself to testing of three-dimensional printed grafts with varied microstructure and composition.¹⁰⁹⁻¹¹²

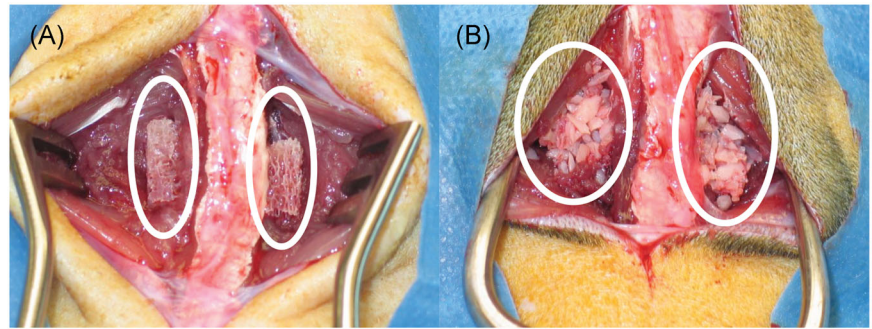
3.3 | Vertebrae

Animal models of *de novo* vertebral bone synthesis are largely divided into two types, vertebral body defects and spinal fusion. In small mammals, vertebral body defects are typically spherical^{113-115,228,229} as in an osteoporotic rat model that showed increased bone formation and improved stiffness of new bone with platelet-rich plasma combined with a gelatin/ β -tricalcium phosphate (TCP) sponge.²³⁰ Both kyphoplasty materials and novel implants are frequently tested in ovine.^{116-119,231,232} Defect models often replicate highly prevalent lumbar (L) 2–5 vertebral body compression fractures. Midbody defects up to 6 mm in diameter and burst fractures created by manual compression are reported in skeletally mature animals with 12–36 weeks postoperative follow up.^{116-122,233} As with all bones, there are important anatomical differences between human and animal vertebrae, however, the immature domestic porcine (55–65 kg) vertebral macrostructure resembles the human in pedicle dimensions,²³⁴ vertebral body height, and end-plate and spinal canal shape.²³⁵ Polymethylmethacrylate cement containing magnets injected into porcine thoracic vertebrae to mimic kyphoplasty attracted systemically administered magnetic nanoparticles.²³⁶ Lumbar posterolateral spinal fusion is modeled in large and small animals, among which the rodent and lapin are commonly used to evaluate *de novo* bone formation and remodeling in a non-instrumented model (Figure 4).²³⁷⁻²⁴⁰ Bilateral decortication of the L4–L5 or L5–L6 transverse processes, with or without decortication of the spinous processes and lamina, produces stable fracture beds to which materials are applied topically. As illustrated by a rat spinal fusion study that showed syngeneic adipose tissue-derived multipotent stromal cells (ASCs) on β -TCP/collagen type I matrix enhanced bone formation over matrix with allogeneic ASCs or matrix alone,²⁴⁰ bone formation is readily assessed with radiographs, μ -CT and routine histology.²³⁷⁻²³⁹

3.4 | Facial Bone

The mandible, orbital, zygoma, maxilla, and frontal bones are frequently sites of congenital malformation and trauma.^{241,242} Facial bone regeneration is somewhat distinct in that minimal soft tissue coverage and esthetics require close replication of the original structure. In the rat model, CSDs in the mandible beneath the pterygomasseteric sling are used to test materials.¹²³⁻¹²⁸ A distinct feature of the rat mandible is absence of a bony symphysis between hemimandibles that reduces load transfer and allows asynchronous motion between them.²⁴³⁻²⁴⁵ Asymmetric masticatory function and dominant and nondominant hemimandibles are described in rats.²⁴⁶ As such random assignment of treatment among hemimandibles or bilateral defects may be more important in rats than other models. Segmental defects in large animal models are frequently reported in the mandible,^{129,130,247-251} hard palate,²⁵²⁻²⁵⁴ and zygoma.¹³¹ Unicortical and bicortical defects consisting of partial and full thickness bone resections are reported throughout the mandible in multiple large animal species including canine, ovine and porcine. Unicortical, partial bone thickness alveolar bone “saddle

FIGURE 4 Demineralized bone matrix (A, white circles) and corticocancellous bone (B, white circles) during implantation in a rat model of lumbar spinal fusion. The lumbar spine is evident between the circles in each image [Color figure can be viewed at wileyonlinelibrary.com]



back” defects are frequently used to test bone regeneration in the unique bone-tooth interface.^{249,255} Stabilization varies with defect size and configuration as does time required for bone healing with 12 weeks typical for canine and ovine and porcine requiring slightly longer.^{129-131,247-251} As in long bones, the best models are in those bones with proportionately similar loading and comparable anatomy to human. In terms of bone volume, trabecular thickness, and trabecular spacing, ovine and porcine mandible are among the closest to human.¹³² Additionally, the porcine temporomandibular micro- and macrostructure resembles that of the human, and the joints in both species experience similar masticatory forces.¹³³ This makes the porcine mandibular condylectomy model well aligned with condyle and ramus regeneration studies.¹³⁰

4 | FUTURE DIRECTIONS

Numerous novel interventions tested in animal models are the foundation on which current standard bone regeneration therapies are based. The future is bright as humanized animal models make it possible to more closely align outcomes between human and non-human species. Further advances may include larger species with bone size, shape and stresses that are similar to human. Continued efforts to identify shared conditions that occur naturally in animals and humans may increase parallel clinical trials, especially for age-related tissue changes. Three-dimensional printing with organic and inorganic materials has limitless possibilities for treatment customization, not only for optimal bone size and shape, but composition and therapeutics. Cellular therapies will be enhanced by mechanisms to control cell migration and measure cell longevity in vivo. These are among the innumerable other ambitious goals that are the basis for discovery efforts that will change the future of health care options.

5 | CONCLUSIONS

The information above provides a limited glimpse of the burgeoning scientific efforts focused on bone restoration. It also highlights that shared goals to improve treatment options benefit all members of our global community. The importance of carefully selected animal models contributes to advances in de novo bone formation daily. This drives

development and translation of targeted therapies that improve the health and well-being of humans and animals alike. The concept of one health has gained renewed attention recently. In a nutshell, the message supports the benefits of sharing discoveries to address medical challenges afflicting numerous species among medical disciplines that attend to them. Naturally, it is vital to both recognize and respect inherent differences among species that limit direct translation of scientific knowledge. Nonetheless, the rapid progress of ex vivo and in vivo de novo bone generation is clearing propelling a wealth of revolutionary innovation to reality among scientific and clinical specialists.

ACKNOWLEDGMENTS

This study is funded in part by the Louisiana State University Equine Health Studies Program and the Tynewald Foundation. The authors thank Dr. Clifford Les for the image in Figure 2.

AUTHOR CONTRIBUTIONS

Mandi J. Lopez conceived the original idea. Takashi Taguchi and Mandi J. Lopez performed the literature search and wrote the manuscript. All authors read and approved the final submitted manuscript.

ORCID

Takashi Taguchi  <http://orcid.org/0000-0001-5790-2003>

Mandi J. Lopez  <https://orcid.org/0000-0002-8776-8594>

REFERENCES

1. Bagi CM, Berryman E, Moalli MR. Comparative bone anatomy of commonly used laboratory animals: implications for drug discovery. *Comp Med*. 2011;61:76-85.
2. Aerssens J, Boonen S, Lowet G, et al. Interspecies differences in bone composition, density, and quality: potential implications for in vivo bone research. *Endocrinology*. 1998;139:663-670.
3. McNeil CJ, Raymer GH, Doherty TJ, et al. Geometry of a weight-bearing and non-weight-bearing bone in the legs of young, old, and very old men. *Calcif Tissue Int*. 2009;85:22-30.
4. Lammens J, Marechal M, Geris L, et al. Warning about the use of critical-size defects for the translational study of bone repair: analysis of a sheep tibial model. *Tissue Eng Part C Methods*. 2017;23:694-699.
5. Malhotra A, Pelletier MH, Yu Y, et al. A sheep model for cancellous bone healing. *Front Surg*. 2014;1:37.
6. Vajgel A, Mardas N, Farias BC, et al. A systematic review on the critical size defect model. *Clin Oral Implants Res*. 2014;25:879-893.

7. Jilka RL. The relevance of mouse models for investigating age-related bone loss in humans. *J Gerontol A Biol Sci Med Sci*. 2013;68:1209-1217.
8. Geiger M, Gendron K, Willmitzer F, et al. Unaltered sequence of dental, skeletal, and sexual maturity in domestic dogs compared to the wolf. *Zoological Lett*. 2016;2:16.
9. Beunen GP, Rogol AD, Malina RM. Indicators of biological maturation and secular changes in biological maturation. *Food Nutr Bull*. 2006;27:S244-256.
10. Sengupta P. The laboratory rat: relating its age with human's. *Int J Prev Med*. 2013;4:624-630.
11. Reiland S. Growth and skeletal development of the pig. *Acta Radiol Suppl*. 1978;358:15-22.
12. Drevon-Gaillot E, Perron-Lepage MF, Clement C, et al. A review of background findings in cynomolgus monkeys (*Macaca fascicularis*) from three different geographical origins. *Exp Toxicol Pathol*. 2006;58:77-88.
13. Masoud I, Shapiro F, Kent R, et al. A longitudinal study of the growth of the New Zealand white rabbit: cumulative and biweekly incremental growth rates for body length, body weight, femoral length, and tibial length. *J Orthop Res*. 1986;4:221-231.
14. Kilborn SH, Trudel G, Uthoff H. Review of growth plate closure compared with age at sexual maturity and lifespan in laboratory animals. *Contemp Top Lab Anim Sci*. 2002;41:21-26.
15. Cech DJ, Martin ST. Skeletal system changes. In: Cech DJ, Martin ST, eds. *Functional Movement Development Across the Life Span*. Saint Louis: W.B. Saunders; 2012:105-128.
16. Moran NC, O'Connor TP. Age attribution in domestic sheep by skeletal and dental maturation: a pilot study of available sources. *Intl J Osteoarchaeol*. 1994;4:267-285.
17. Colman RJ, Lane MA, Binkley N, et al. Skeletal effects of aging in male rhesus monkeys. *Bone*. 1999;24:17-23.
18. Silverman S, Morgan JP, Ferron R, et al. Radiographic evaluation of appendicular skeletal maturation in the rhesus-monkey. *Vet Radiol*. 1983;24:25-34.
19. Pfeifer CG, Fisher MB, Saxena V, et al. Age-dependent subchondral bone remodeling and cartilage repair in a minipig defect model. *Tissue Eng Part C Methods*. 2017;23:745-753.
20. Bode G, Clausing P, Gervais F, et al. The utility of the minipig as an animal model in regulatory toxicology. *J Pharmacol Toxicol Methods*. 2010;62:196-220.
21. Strand E, Braathen LC, Hellsten MC, et al. Radiographic closure time of appendicular growth plates in the Icelandic horse. *Acta Vet Scand*. 2007;49:19.
22. Hillier ML, Bell LS. Differentiating human bone from animal bone: a review of histological methods. *J Forensic Sci*. 2007;52:249-263.
23. Skedros JG, Keenan KE, Williams TJ, et al. Secondary osteon size and collagen/lamellar organization ("osteon morphotypes") are not coupled, but potentially adapt independently for local strain mode or magnitude. *J Struct Biol*. 2013;181:95-107.
24. Saha S, Hayes WC. Relations between tensile impact properties and microstructure of compact bone. *Calcif Tissue Res*. 1977;24:65-72.
25. Wang X, Mabrey JD, Agrawal CM. An interspecies comparison of bone fracture properties. *Biomed Mater Eng*. 1998;8:1-9.
26. Skedros JG, Kiser CJ, Keenan KE, et al. Analysis of osteon morphotype scoring schemes for interpreting load history: evaluation in the chimpanzee femur. *J Anat*. 2011;218:480-499.
27. Mason MW, Skedros JG, Bloebaum RD. Evidence of strain-mode-related cortical adaptation in the diaphysis of the horse radius. *Bone*. 1995;17:229-237.
28. Vajda EG, Kneissel M, Muggenburg B, et al. Increased intracortical bone remodeling during lactation in beagle dogs. *Biol Reprod*. 1999;61:1439-1444.
29. Dannucci GA, Martin RB, Patterson-Buckendahl P. Ovariectomy and trabecular bone remodeling in the dog. *Calcif Tissue Int*. 1987;40:194-199.
30. Vignery A, Baron R. Dynamic histomorphometry of alveolar bone remodeling in the adult rat. *Anat Rec*. 1980;196:191-200.
31. Delmas PD, Vergnaud P, Arlot ME, et al. The anabolic effect of human PTH (1-34) on bone formation is blunted when bone resorption is inhibited by the bisphosphonate tiludronate—is activated resorption a prerequisite for the in vivo effect of PTH on formation in a remodeling system? *Bone*. 1995;16:603-610.
32. McNulty PA, Dayan AD, Ganderup N-C, et al. *The Minipig in Biomedical Research*. CRC Press; 2011.
33. Mashiba T, Burr DB, Turner CH, et al. Effects of human parathyroid hormone (1-34), LY333334, on bone mass, remodeling, and mechanical properties of cortical bone during the first remodeling cycle in rabbits. *Bone*. 2001;28:538-547.
34. Motyl KJ, Dick-de-Paula I, Maloney AE, et al. Trabecular bone loss after administration of the second-generation antipsychotic risperidone is independent of weight gain. *Bone*. 2012;50:490-498.
35. Cheng S, Aghajanian P, Pourteymoor S, et al. Prolyl hydroxylase domain-containing protein 2 (Phd2) regulates chondrocyte differentiation and secondary ossification in mice. *Sci Rep*. 2016;6:35748.
36. Nallamshetty S, Wang H, Rhee EJ, et al. Deficiency of retinaldehyde dehydrogenase 1 induces BMP2 and increases bone mass in vivo. *PLOS One*. 2013;8:e71307.
37. Huja SS, Fernandez SA, Hill KJ, et al. Remodeling dynamics in the alveolar process in skeletally mature dogs. *Anat Rec A Discov Mol Cell Evol Biol*. 2006;288:1243-1249.
38. Forwood MR, Burr DB, Takano Y, et al. Risedronate treatment does not increase microdamage in the canine femoral neck. *Bone*. 1995;16:643-650.
39. Tanizawa T, Itoh A, Uchiyama T, et al. Changes in cortical width with bone turnover in the three different endosteal envelopes of the ilium in postmenopausal osteoporosis. *Bone*. 1999;25:493-499.
40. Clarke B. Normal bone anatomy and physiology. *Clin J Am Soc Nephrol*. 2008;3(suppl 3):S131-S139.
41. Manolagas SC. Birth and death of bone cells: basic regulatory mechanisms and implications for the pathogenesis and treatment of osteoporosis. *Endocr Rev*. 2000;21:115-137.
42. Rubin C, Xu G, Judex S. The anabolic activity of bone tissue, suppressed by disuse, is normalized by brief exposure to extremely low-magnitude mechanical stimuli. *FASEB J*. 2001;15:2225-2229.
43. Recker RR, Kimmel DB, Parfitt AM, et al. Static and tetracycline-based bone histomorphometric data from 34 normal postmenopausal females. *J Bone Miner Res*. 1988;3:133-144.
44. Shahnazari M, Burr DB, Lee WH, et al. Cross-calibration of 45calcium kinetics against dynamic histomorphometry in a rat model to determine bone turnover. *Bone*. 2010;46:1238-1243.
45. Newman E, Turner AS, Wark JD. The potential of sheep for the study of osteopenia: current status and comparison with other animal models. *Bone*. 1995;16:2775-2845.
46. Balena R, Toolan BC, Shea M, et al. The effects of 2-year treatment with the aminobisphosphonate alendronate on bone metabolism, bone histomorphometry, and bone strength in ovariectomized nonhuman primates. *J Clin Invest*. 1993;92:2577-2586.
47. Lees CJ, Ramsay H. Histomorphometry and bone biomarkers in cynomolgus females: a study in young, mature, and old monkeys. *Bone*. 1999;24:25-28.
48. Da Costa Gomez TM, Barrett JG, Sample SJ, et al. Up-regulation of site-specific remodeling without accumulation of microcracking and loss of osteocytes. *Bone*. 2005;37:16-24.
49. Reifenrath J, Gottschalk D, Angrisani N, et al. Axial forces and bending moments in the loaded rabbit tibia in vivo. *Acta Vet Scand*. 2012;54:21.

50. Weinans H, Blankevoort L. Reconstruction of bone loading conditions from in vivo strain measurements. *J Biomech.* 1995;28:739-744.
51. Shahar R, Banks-Sills L. Biomechanical analysis of the canine hind limb: calculation of forces during three-legged stance. *Vet J.* 2002; 163:240-250.
52. Wehner T, Claes L, Simon U. Internal loads in the human tibia during gait. *Clin Biomech.* 2009;24:299-302.
53. Taylor WR, Ehrig RM, Heller MO, et al. Tibio-femoral joint contact forces in sheep. *J Biomech.* 2006;39:791-798.
54. Im JY, Min WK, You C, et al. Bone regeneration of mouse critical-sized calvarial defects with human mesenchymal stem cells in scaffold. *Lab Anim Res.* 2013;29:196-203.
55. Zhang Y, Wang L, Deng F, et al. Determination of a critical size calvarial defect in senile osteoporotic mice model based on in vivo micro-computed tomography and histological evaluation. *Arch Gerontol Geriatr.* 2015;61:44-55.
56. Suenaga H, Furukawa KS, Suzuki Y, et al. Bone regeneration in calvarial defects in a rat model by implantation of human bone marrow-derived mesenchymal stromal cell spheroids. *J Mater Sci Mater Med.* 2015;26:254.
57. Liu R, Qiao W, Huang B, et al. Fluorination enhances the osteogenic capacity of Porcine hydroxyapatite. *Tissue Eng Part A.* 2018; 24:1207-1217.
58. Hobar PC, Schreiber JS, McCarthy JG, et al. The role of the dura in cranial bone regeneration in the immature animal. *Plast Reconstr Surg.* 1993;92:405-410.
59. Salamanca E, Hsu CC, Huang HM, et al. Bone regeneration using a porcine bone substitute collagen composite in vitro and in vivo. *Sci Rep.* 2018;8:984.
60. Fujioka-Kobayashi M, Kobayashi E, Schaller B, et al. Effect of recombinant human bone morphogenic protein 9 (rhBMP9) loaded onto bone grafts versus barrier membranes on new bone formation in a rabbit calvarial defect model. *J Biomed Mater Res A.* 2017; 105:2655-2661.
61. Umeda H, Kanemaru S, Yamashita M, et al. Bone regeneration of canine skull using bone marrow-derived stromal cells and beta-tricalcium phosphate. *Laryngoscope.* 2007;117:997-1003.
62. Liu G, Zhang Y, Liu B, et al. Bone regeneration in a canine cranial model using allogeneic adipose derived stem cells and coral scaffold. *Biomaterials.* 2013;34:2655-2664.
63. Gerety PA, Wink JD, Sherif RD, et al. Treatment of large calvarial defects with bone transport osteogenesis: a preclinical sheep model. *J Craniofacial Surg.* 2014;25:1917-1922.
64. Kramer FJ, Mueller M, Rahmstorf M, et al. Ortho- and heterotopic bone grafts in bifocal transport osteogenesis for craniofacial reconstruction—an experimental study in sheep. *Int J Oral Maxillofac Surg.* 2004;33:575-583.
65. Blaszczyk B, Kaspera W, Ficek K, et al. Effects of polylactide copolymer implants and platelet-rich plasma on bone regeneration within a large calvarial defect in sheep. *Biomed Res Int.* 2018;2018: 4120471.
66. Cao Y, Xiong J, Mei S, et al. Aspirin promotes bone marrow mesenchymal stem cell-based calvarial bone regeneration in mini swine. *Stem Cell Res Ther.* 2015;6:210.
67. Rolfing JH, Jensen J, Jensen JN, et al. A single topical dose of erythropoietin applied on a collagen carrier enhances calvarial bone healing in pigs. *Acta Orthop.* 2014;85:201-209.
68. Hoshino M, Egi T, Terai H, et al. Regenerative repair of long intercalated rib defects using porous cylinders of beta-tricalcium phosphate: an experimental study in a canine model. *Plast Reconstr Surg.* 2007;119:1431-1439.
69. Tang H, Xu Z, Qin X, et al. Chest wall reconstruction in a canine model using polydioxanone mesh, demineralized bone matrix and bone marrow stromal cells. *Biomaterials.* 2009;30:3224-3233.
70. Wilson TA, Rehder K, Krayner S, et al. Geometry and respiratory displacement of human ribs. *J Appl Physiol.* 1985;62:1872-1877.
71. Margulies SS, Rodarte JR, Hoffman EA. Geometry and kinematics of dog ribs. *J Appl Physiol.* 1985;67:707-712.
72. Chang DW, Satterfield WC, Son D, et al. Use of vascularized periosteum or bone to improve healing of segmental allografts after tumor resection: an ovine rib model. *Plast Reconstr Surg.* 2009;123:71-78.
73. Zhang R, Magel L, Jonigk D, et al. Biosynthetic nanostructured cellulose patch for chest wall reconstruction: five-month follow-up in a Porcine model. *J Invest Surg.* 2017;30:297-302.
74. Huri PY, Huri G, Yasar U, et al. A biomimetic growth factor delivery strategy for enhanced regeneration of iliac crest defects. *Biomed Mater.* 2013;8:045009.
75. Tian XF, Heng BC, Ge Z, et al. Comparison of osteogenesis of human embryonic stem cells within 2D and 3D culture systems. *Scand J Clin Lab Invest.* 2008;68:58-67.
76. Alt V, Cheung WH, Chow SK, et al. Bone formation and degradation behavior of nanocrystalline hydroxyapatite with or without collagen-type 1 in osteoporotic bone defects—an experimental study in osteoporotic goats. *Injury.* 2016;47(suppl 2):S58-65.
77. Kruyt MC, Dhert WJ, Yuan H, et al. Bone tissue engineering in a critical size defect compared to ectopic implantations in the goat. *J Orthop Res.* 2004;22:544-551.
78. Anderson ML, Dhert WJ, Bruijn JD, et al. Critical size defect in the goat's os ilium. A model to evaluate bone grafts and substitutes. *Clin Orthop Relat Res.* 1999:231-239.
79. Kaempfen A, Todorov A, Guven S, et al. Engraftment of prevascularized, tissue engineered constructs in a novel rabbit segmental bone defect model. *Int J Mol Sci.* 2015;16:12616-12630.
80. Murakami N, Saito N, Horiuchi H, et al. Repair of segmental defects in rabbit humeri with titanium fiber mesh cylinders containing recombinant human bone morphogenetic protein-2 (rhBMP-2) and a synthetic polymer. *J Biomed Mater Res.* 2002;62:169-174.
81. Kohler P, Ehrnberg A, Kreicbergs A. Osteogenic enhancement of diaphyseal reconstruction: comparison of bone grafts in the rabbit. *Acta Orthop Scand.* 1990;61:42-45.
82. Rhodes NP, Hunt JA, Longinotti C, et al. In vivo characterization of Hyalonect, a novel biodegradable surgical mesh. *J Surg Res.* 2011;168: e31-38.
83. Faria PE, Carvalho AL, Felipucci DN, et al. Bone formation following implantation of titanium sponge rods into humeral osteotomies in dogs: a histological and histometrical study. *Clin Implant Dent Relat Res.* 2010;12:72-79.
84. Sumner DR, Turner TM, Cohen M, et al. Aging does not lessen the effectiveness of TGFbeta2-enhanced bone regeneration. *J Bone Miner Res.* 2003;18:730-736.
85. Luneva SN, Talashova IA, Osipova EV, et al. Effects of composition of biocomposite materials implanted into hole defects of the metaphysis on the reparative regeneration and mineralization of bone tissue. *Bull Exp Biol Med.* 2013;156:285-289.
86. Turner TM, Urban RM, Hall DJ, et al. Local and systemic levels of tobramycin delivered from calcium sulfate bone graft substitute pellets. *Clin Orthop Relat Res.* 2005:97-104.
87. Pobloth AM, Johnson KA, Schell H, et al. Establishment of a pre-clinical ovine screening model for the investigation of bone tissue engineering strategies in cancellous and cortical bone defects. *BMC Musculoskelet Disord.* 2016;17:111.
88. Uebersax L, Apfel T, Nuss KM, et al. Biocompatibility and osteoconduction of macroporous silk fibroin implants in cortical defects in sheep. *Eur J Pharm Biopharm.* 2013;85:107-118.
89. Nuss KM, Auer JA, Boos A, et al. An animal model in sheep for biocompatibility testing of biomaterials in cancellous bones. *BMC Musculoskelet Disord.* 2006;7:67.

90. Meimandi-Parizi A, Oryan A, Bigham-Sadegh A, et al. Effects of chitosan scaffold along with royal jelly or bee venom in regeneration of critical sized radial bone defect in rat. *Iran J Vet Res.* 2018;19:246-254.
91. Oryan A, Alidadi S, Bigham-Sadegh A, et al. Healing potentials of polymethylmethacrylate bone cement combined with platelet gel in the critical-sized radial bone defect of rats. *PLOS One.* 2018;13:e0194751.
92. Wang ZX, Chen C, Zhou Q, et al. The treatment efficacy of bone tissue engineering strategy for repairing segmental bone defects under osteoporotic conditions. *Tissue Eng Part A.* 2015;21:2346-2355.
93. Zhao MD, Huang JS, Zhang XC, et al. Construction of radial defect models in rabbits to determine the critical size defects. *PLOS One.* 2016;11:e0146301.
94. Zhao L, Zhao J, Wang S, et al. Comparative study between tissue-engineered periosteum and structural allograft in rabbit critical-sized radial defect model. *J Biomed Mater Res B Appl Biomater.* 2011;97:1-9.
95. Lane JM, Sandhu HS. Current approaches to experimental bone grafting. *Orthop Clin North Am.* 1987;18:213-225.
96. Sharifi D, Khoushkerdar HR, Abedi G, et al. Mechanical properties of radial bone defects treated with autogenous graft covered with hydroxyapatite in rabbit. *Acta Cir Bras.* 2012;27:256-259.
97. Yilmaz O, Ozmeric A, Alemdaroglu KB, et al. Effects of concentrated growth factors (CGF) on the quality of the induced membrane in Masquelet's technique—an experimental study in rabbits. *Injury.* 2018;49:1497-1503.
98. Witek L, Alifarag AM, Tovar N, et al. Repair of critical-sized long bone defects using dipyrindamole-augmented 3D-printed bioactive ceramic scaffolds. *J Orthop Res.* 2019;37:2499-2507.
99. Saxer F, Scherberich A, Todorov A, et al. Implantation of stromal vascular fraction progenitors at bone fracture sites: from a rat model to a first-in-man study. *Stem Cells.* 2016;34:2956-2966.
100. Montijo HE, Kellam JF, Gettys FK, et al. Utilization of the AO LockingRatNail in a novel rat femur critical defect model. *J Invest Surg.* 2012;25:381-386.
101. Angle SR, Sena K, Sumner DR, et al. Healing of rat femoral segmental defect with bone morphogenetic protein-2: a dose response study. *J Musculoskelet Neuronal Interact.* 2012;12:28-37.
102. Jager M, Sager M, Lensing-Hohn S, et al. The critical size bony defect in a small animal for bone healing studies (II): implant evolution and surgical technique on a rat's femur. *Biomed Tech.* 2005;50:137-142.
103. Shen HC, Peng H, Usas A, et al. Structural and functional healing of critical-size segmental bone defects by transduced muscle-derived cells expressing BMP4. *J Gene Med.* 2004;6:984-991.
104. Fukuroku J, Inoue N, Rafiee B, et al. Extracortical bone-bridging fixation with use of cortical allograft and recombinant human osteogenic protein-1. *J Bone Joint Surg Am.* 2007;89:1486-1496.
105. Johnson AL, Shokry MM, Stein LE. Preliminary study of ethylene oxide sterilization of full-thickness cortical allografts used in segmental femoral fracture repair. *Am J Vet Res.* 1985;46:1050-1056.
106. Zabka AG, Pluhar GE, Edwards RB, et al. Histomorphometric description of allograft bone remodeling and union in a canine segmental femoral defect model: a comparison of rhBMP-2, cancellous bone graft, and absorbable collagen sponge. *J Orthop Res.* 2001;19:318-327.
107. Kraus KH, Kadiyala S, Wotton H, et al. Critically sized osteo-periosteal femoral defects: a dog model. *J Invest Surg.* 1999;12:115-124.
108. Nather A, David V, Teng JW, et al. Effect of autologous mesenchymal stem cells on biological healing of allografts in critical-sized tibial defects simulated in adult rabbits. *Ann Acad Med Singapore.* 2010;39:599-606.
109. Pobloth AM, Schell H, Petersen A, et al. Tubular open-porous beta-tricalcium phosphate polycaprolactone scaffolds as guiding structure for segmental bone defect regeneration in a novel sheep model. *J Tissue Eng Regen Med.* 2018;12:897-911.
110. Ben-David D, Fishman B, Rubin G, et al. Autologous cell-coated particles for the treatment of segmental bone defects—a new cell therapy approach. *J Orthop Surg Res.* 2019;14:198.
111. Li JJ, Dunstan CR, Entezari A, et al. A novel bone substitute with high bioactivity, strength, and porosity for repairing large and load-bearing bone defects. *Adv Healthc Mater.* 2019;8:e1801298.
112. Berner A, Henkel J, Woodruff MA, et al. Delayed minimally invasive injection of allogenic bone marrow stromal cell sheets regenerates large bone defects in an ovine preclinical animal model. *Stem Cells Transl Med.* 2015;4:503-512.
113. Liang H, Wang K, Shimer AL, et al. Use of a bioactive scaffold for the repair of bone defects in a novel reproducible vertebral body defect model. *Bone.* 2010;47:197-204.
114. Shen GY, Ren H, Tang JJ, et al. Effect of osteoporosis induced by ovariectomy on vertebral bone defect/fracture in rat. *Oncotarget.* 2017;8:73559-73567.
115. Sakata M, Tonomura H, Itsuji T, et al. Osteoporotic effect on bone repair in lumbar vertebral body defects in a rat model. *J Orthop Surg.* 2018;26:2309499018770349.
116. James AW, Chiang M, Asatrian G, et al. Vertebral implantation of NELL-1 enhances bone formation in an osteoporotic sheep model. *Tissue Eng Part A.* 2016;22:840-849.
117. Yang HL, Zhu XS, Chen L, et al. Bone healing response to a synthetic calcium sulfate/beta-tricalcium phosphate graft material in a sheep vertebral body defect model. *J Biomed Mater Res B Appl Biomater.* 2012;100:1911-1921.
118. Kobayashi H, Fujishiro T, Belkoff SM, et al. Long-term evaluation of a calcium phosphate bone cement with carboxymethyl cellulose in a vertebral defect model. *J Biomed Mater Res A.* 2009;88:880-888.
119. Fujishiro T, Bauer TW, Kobayashi N, et al. Histological evaluation of an impacted bone graft substitute composed of a combination of mineralized and demineralized allograft in a sheep vertebral bone defect. *J Biomed Mater Res A.* 2007;82:538-544.
120. Zhu X, Chen X, Chen C, et al. Evaluation of calcium phosphate and calcium sulfate as injectable bone cements in sheep vertebrae. *J Spinal Disord Tech.* 2012;25:333-337.
121. Zhu XS, Zhang ZM, Mao HQ, et al. A novel sheep vertebral bone defect model for injectable bioactive vertebral augmentation materials. *J Mater Sci Mater Med.* 2011;22:159-164.
122. Wang Z, Lu B, Chen L, et al. Evaluation of an osteostimulative putty in the sheep spine. *J Mater Sci Mater Med.* 2011;22:185-191.
123. Miller MQ, McColl LF, Arul MR, et al. Assessment of Hedgehog signaling pathway activation for craniofacial bone regeneration in a critical-sized rat mandibular defect. *JAMA Facial Plast Surg.* 2019; 21:110-117.
124. Baskin JZ, Soenjaya Y, McMasters J, et al. Nanophase bone substitute for craniofacial load bearing application: Pilot study in the rodent. *J Biomed Mater Res B Appl Biomater.* 2018;106:520-532.
125. Jorge RS, Jorge J Jr., Luz JG. Reconstruction of a mandibular critical-sized defect using iliac graft in rats. *Implant Dent.* 2006;15:282-289.
126. Kowalczewski CJ, Tombyln S, Wasnick DC, et al. Reduction of ectopic bone growth in critically-sized rat mandible defects by delivery of rhBMP-2 from keratins biomaterials. *Biomaterials.* 2014;35:3220-3228.
127. Saadeh PB, Khosla RK, Mehrara BJ, et al. Repair of a critical size defect in the rat mandible using allogenic type I collagen. *J Craniofac Surg.* 2001;12:573-579.
128. Bhattarai G, Kook SH, Kim JH, et al. COMP-Ang1 prevents periodontitis damages and enhances mandible bone growth in an experimental animal model. *Bone.* 2016;92:168-179.
129. Zhang W, Abukawa H, Troulis MJ, et al. Tissue engineered hybrid tooth-bone constructs. *Methods.* 2009;47:122-128.
130. Bhumiratana S, Bernhard JC, Alfi DM, et al. Tissue-engineered autologous grafts for facial bone reconstruction. *Sci Transl Med.* 2016;8:343ra383.

131. Mulloy C, Guidry RF, Sharma S, et al. Experimental model of zygomatic and mandibular defects to support the development of custom three-dimensional—printed bone scaffolds. *J Craniofac Surg.* 2020;31(5):1488-1491.
132. Watson PJ, Fitton LC, Meloro C, et al. Mechanical adaptation of trabecular bone morphology in the mammalian mandible. *Sci Rep.* 2018;8:7277.
133. Herring SW. TMJ anatomy and animal models. *J Musculoskelet Neuronal Interact.* 2003;3(4):391-394.
134. Skedros JG, Su SC, Bloebaum RD. Biomechanical implications of mineral content and microstructural variations in cortical bone of horse, elk, and sheep calcanei. *Anat Rec.* 1997;249:297-316.
135. Christen P, Ito K, Ellouz R, et al. Bone remodelling in humans is load-driven but not lazy. *Nat Commun.* 2014;5:4855.
136. Hart NH, Nimphius S, Rantalainen T, et al. Mechanical basis of bone strength: influence of bone material, bone structure and muscle action. *J Musculoskelet Neuronal Interact.* 2017;17:114-139.
137. Skedros JG, Sorenson SM, Jenson NH. Are distributions of secondary osteon variants useful for interpreting load history in mammalian bones? *Cells Tissues Organs.* 2007;185:285-307.
138. Taylor ME, Tanner KE, Freeman MAR, et al. Stress and strain distribution within the intact femur: compression or bending. *Med Eng Phys.* 1996;18:122-131.
139. Duda GN, Schneider E, Chao EY. Internal forces and moments in the femur during walking. *J Biomech.* 1997;30:933-941.
140. Shahar R, Banks-Sills L, Eliasy R. Stress and strain distribution in the intact canine femur: finite element analysis. *Med Eng Phys.* 2003;25:387-395.
141. Simmons T, Goodburn B, Singhrao SK. Decision tree analysis as a supplementary tool to enhance histomorphological differentiation when distinguishing human from non-human cranial bone in both burnt and unburnt states: a feasibility study. *Med Sci Law.* 2016;56:36-45.
142. Nganvongpanit K, Pradit W, Pitakarnnop T, et al. Differences in osteon structure histomorphometry between puppyhood and adult stages in the golden retriever. *Anat Sci Int.* 2017;92:483-492.
143. Stover SM, Pool RR, Martin RB, et al. Histological features of the dorsal cortex of the third metacarpal bone mid-diaphysis during postnatal growth in thoroughbred horses. *J Anat.* 1992;181(pt 3):455-469.
144. Mori R, Kodaka T, Sano T, et al. Comparative histology of the laminar bone between young calves and foals. *Cells Tissues Organs.* 2003;175:43-50.
145. Felder AA, Phillips C, Cornish H, et al. Secondary osteons scale allometrically in mammalian humerus and femur. *R Soc Open Sci.* 2017;4:170431.
146. Dempster DW, Compston JE, Drezner MK, et al. Standardized nomenclature, symbols, and units for bone histomorphometry: a 2012 update of the report of the ASBMR Histomorphometry Nomenclature Committee. *J Bone Miner Res.* 2013;28:2-17.
147. Recker RR, Ste-Marie LG, Langdahl B, et al. Effects of intermittent intravenous ibandronate injections on bone quality and micro-architecture in women with postmenopausal osteoporosis: the DIVA study. *Bone.* 2010;46:660-665.
148. Essen HW, Holzmann PJ, Blankenstein MA, et al. Effect of raloxifene treatment on osteocyte apoptosis in postmenopausal women. *Calcif Tissue Int.* 2007;81:183-190.
149. Rehman MT, Hoyland JA, Denton J, et al. Age related histomorphometric changes in bone in normal British men and women. *J Clin Pathol.* 1994;47:529-534.
150. Mori T, Okimoto N, Sakai A, et al. Climbing exercise increases bone mass and trabecular bone turnover through transient regulation of marrow osteogenic and osteoclastogenic potentials in mice. *J Bone Miner Res.* 2003;18:2002-2009.
151. Chen S, Liu D, He S, et al. Differential effects of type 1 diabetes mellitus and subsequent osteoblastic beta-catenin activation on trabecular and cortical bone in a mouse model. *Exp Mol Med.* 2018;50:1-14.
152. Slatopolsky E, Cozzolino M, Lu Y, et al. Efficacy of 19-Nor-1,25-(OH)₂D₂ in the prevention and treatment of hyperparathyroid bone disease in experimental uremia. *Kidney Int.* 2003;63:2020-2027.
153. Xu J, Wang B, Sun Y, et al. Human fetal mesenchymal stem cell secretome enhances bone consolidation in distraction osteogenesis. *Stem Cell Res Ther.* 2016;7:134.
154. Lu H, Cui L, Zuo C, et al. Evaluation of morphological parameters of bone formation in Sprague-Dawley rats of different ages by in vivo fluorochrome labeling. *Italian J Zoo.* 2015;82:33-40.
155. Kondo E, Yasoda A, Fujii T, et al. Increased bone turnover and possible accelerated fracture healing in a Murine model with an increased circulating C-type natriuretic peptide. *Endocrinology.* 2015;156:2518-2529.
156. Connolly JF, Hahn H, Davy D. Fracture healing in weight-bearing and nonweight-bearing bones. *J Trauma.* 1978;18:766-770.
157. Lim J, Lee J, Yun H-S, et al. Comparison of bone regeneration rate in flat and long bone defects: Calvarial and tibial bone. *Tissue Eng Regen Med.* 2013;10:336-340.
158. Levi B, Nelson ER, Li S, et al. Dura mater stimulates human adipose-derived stromal cells to undergo bone formation in mouse calvarial defects. *Stem Cells.* 2011;29:1241-1255.
159. Mizuno H, Kikuta J, Ishii M. In vivo live imaging of bone cells. *Histochem Cell Biol.* 2018;149:417-422.
160. Villa MM, Wang L, Huang J, et al. Visualizing osteogenesis in vivo within a cell-scaffold construct for bone tissue engineering using two-photon microscopy. *Tissue Eng Part C Methods.* 2013;19:839-849.
161. Jensen J, Tvedesøe C, Rølfing JHD, et al. Dental pulp-derived stromal cells exhibit a higher osteogenic potency than bone marrow-derived stromal cells in vitro and in a porcine critical-size bone defect model. *SICOT-J.* 2016;2:16-16..
162. Vila PM, Jeanpierre LM, Rizzi CJ, et al. Comparison of autologous vs homologous costal cartilage grafts in dorsal augmentation rhinoplasty: a systematic review and meta-analysis. *JAMA Otolaryngol Head Neck Surg.* 2020;146(4):347-354.
163. Brown JS, Lowe D, Kanatas A, et al. Mandibular reconstruction with vascularised bone flaps: a systematic review over 25 years. *Br J Oral Maxillofac Surg.* 2017;55:113-126.
164. Weyant MJ, Bains MS, Venkatraman E, et al. Results of chest wall resection and reconstruction with and without rigid prosthesis. *Ann Thorac Surg.* 2006;81:279-285.
165. Liu F, Chen K, Hou L, et al. Determining the critical size of a rabbit rib segmental bone defect model. *Regenerative biomaterials.* 2016;3:323-328.
166. Ishihara A, Zekas LJ, Weisbrode SE, et al. Comparative efficacy of dermal fibroblast-mediated and direct adenoviral bone morphogenetic protein-2 gene therapy for bone regeneration in an equine rib model. *Gene Ther.* 2010;17:733-744.
167. Tataru AM, Shah SR, Demian N, et al. Reconstruction of large mandibular defects using autologous tissues generated from in vivo bioreactors. *Acta Biomater.* 2016;45:72-84.
168. Tataru AM, Koons GL, Watson E, et al. Biomaterials-aided mandibular reconstruction using in vivo bioreactors. *Proc Natl Acad Sci USA.* 2019;116:6954-6963.
169. Liu FZ, Wang DW, Zhang YJ, et al. Comparison of rabbit rib defect regeneration with and without graft. *J Mater Sci Mater Med.* 2017;28:2.
170. Callison WE, Holowka NB, Lieberman DE. Thoracic adaptations for ventilation during locomotion in humans and other mammals. *J Exp Biol.* 2019;222:jeb189357.
171. De Troyer A, Wilson TA. Action of the isolated canine diaphragm on the lower ribs at high lung volumes. *J Physiol.* 2014;592:4481-4491.

172. De Troyer A, Legrand A, Wilson TA. Respiratory mechanical advantage of the canine external and internal intercostal muscles. *J Physiol*. 1999;518:283-289.
173. Thomsen JS, Ebbesen EN, Mosekilde L. Static histomorphometry of human iliac crest and vertebral trabecular bone: a comparative study. *Bone*. 2002;30:267-274.
174. Giavaresi G, Fini M, Martini L, et al. Histomorphometric characterization of cancellous and cortical bone in an ovariectomized sheep model. *J Appl Animal Res*. 2001;20:221-232.
175. Gogolewski S, Gorna K, Turner AS. Regeneration of bicortical defects in the iliac crest of estrogen-deficient sheep, using new biodegradable polyurethane bone graft substitutes. *J Biomed Mater Res A*. 2006;77:802-810.
176. Egermann M, Goldhahn J, Holz R, et al. A sheep model for fracture treatment in osteoporosis: benefits of the model versus animal welfare. *Lab Anim*. 2008;42:453-464.
177. Engelstad ME, Morse T. Anterior iliac crest, posterior iliac crest, and proximal tibia donor sites: a comparison of cancellous bone volumes in fresh cadavers. *J Oral Maxillofac Surg*. 2010;68:3015-3021.
178. Boone DW. Complications of iliac crest graft and bone grafting alternatives in foot and ankle surgery. *Foot Ankle Clin*. 2003;8:1-14.
179. Pohlmeier K, Schmelzeisen R, Botel C. Anatomical basis for transplantation of microsurgical anastomosed autologous and allogenic bone transplantants for reconstruction of the mandible in animal experiments (Gottingen-Minipig). *Anat Anz*. 1990;171:221-226.
180. Lei P, Du W, Liu H, et al. Free vascularized iliac bone flap based on deep circumflex iliac vessels graft for the treatment of osteonecrosis of femoral head. *J Orthop Surg Res*. 2019;14:397.
181. Urbankova I, Vdoviakova K, Rynkevicius R, et al. Comparative anatomy of the ovine and female pelvis. *Gynecol Obstet Invest*. 2017;82:582-591.
182. Meling T, Harboe K, Soreide K. Incidence of traumatic long-bone fractures requiring in-hospital management: a prospective age- and gender-specific analysis of 4890 fractures. *Injury*. 2009;40:1212-1219.
183. Joeris A, Lutz N, Wicki B, et al. An epidemiological evaluation of pediatric long bone fractures—a retrospective cohort study of 2716 patients from two Swiss tertiary pediatric hospitals. *BMC Pediatr*. 2014;14:314.
184. Scholes S, Panesar S, Shelton NJ, et al. Epidemiology of lifetime fracture prevalence in England: a population study of adults aged 55 years and over. *Age Ageing*. 2014;43:234-240.
185. Iwasashi M, Funayama T, Watanabe A, et al. Bone regeneration and remodeling within a unidirectional porous hydroxyapatite bone substitute at a cortical bone defect site: histological analysis at one and two years after implantation. *Materials*. 2015;8:4884-4894.
186. Huffer WE, Benedict JJ, Turner AS, et al. Repair of sheep long bone cortical defects filled with COLLOSS, COLLOSS E, OSSAPLAST, and fresh iliac crest autograft. *J Biomed Mater Res B Appl Biomater*. 2007;82:460-470.
187. Meadows TH, Bronk JT, Chao YS, et al. Effect of weight-bearing on healing of cortical defects in the canine tibia. *J Bone Joint Surg Am*. 1990;72:1074-1080.
188. Herten M, Zilkens C, Thorey F, et al. Biomechanical stability and osteogenesis in a tibial bone defect treated by autologous ovine cord blood cells—a pilot study. *Molecules*. 2019;24(2):295.
189. Street J, Bao M, deGuzman L, et al. Vascular endothelial growth factor stimulates bone repair by promoting angiogenesis and bone turnover. *Proc Natl Acad Sci USA*. 2002;99:9656-9661.
190. Zhang H, Shi X, Wang L, et al. Intramembranous ossification and endochondral ossification are impaired differently between glucocorticoid-induced osteoporosis and estrogen deficiency-induced osteoporosis. *Sci Rep*. 2018;8:3867.
191. Arens D, Wilke M, Calabro L, et al. A rabbit humerus model of plating and nailing osteosynthesis with and without Staphylococcus aureus osteomyelitis. *Eur Cell Mater*. 2015;30:148-161.
192. Fernandes MB, Guimaraes JA, Casado PL, et al. The effect of bone allografts combined with bone marrow stromal cells on the healing of segmental bone defects in a sheep model. *BMC Vet Res*. 2014;10:36.
193. Pobloth AM, Checa S, Razi H, et al. Mechanobiologically optimized 3D titanium-mesh scaffolds enhance bone regeneration in critical segmental defects in sheep. *Sci Transl Med*. 2018;8:28.
194. Christou C, Oliver RA, Pelletier MH, et al. Ovine model for critical-size tibial segmental defects. *Comp Med*. 2014;64:377-385.
195. Runyan CM, Vu AT, Rumburg A, et al. Repair of a critical porcine tibial defect by means of allograft revitalization. *Plast Reconstr Surg*. 2015;136:461e-473e.
196. Southam BR, Archdeacon MT. "Iatrogenic" segmental defect: how I debride high-energy open tibial fractures. *J Orthop Trauma*. 2017;31(suppl 5):S9-S15.
197. Liebschner MA. Biomechanical considerations of animal models used in tissue engineering of bone. *Biomaterials*. 2004;25:1697-1714.
198. Liu C, Cabahug-Zuckerman P, Stubbs C, et al. Mechanical loading promotes the expansion of primitive osteoprogenitors and organizes matrix and vascular morphology in long bone defects. *J Bone Miner Res*. 2019;34:896-910.
199. Liu C, Carrera R, Flamini V, et al. Effects of mechanical loading on cortical defect repair using a novel mechanobiological model of bone healing. *Bone*. 2018;108:145-155.
200. Collet P, Uebelhart D, Vico L, et al. Effects of 1- and 6-month spaceflight on bone mass and biochemistry in two humans. *Bone*. 1997;20:547-551.
201. Vico L, Collet P, Guignandon A, et al. Effects of long-term microgravity exposure on cancellous and cortical weight-bearing bones of cosmonauts. *Lancet*. 2000;355:1607-1611.
202. Giszter SF, Davies MR, Graziani V. Coordination strategies for limb forces during weight-bearing locomotion in normal rats, and in rats spinalized as neonates. *Exp Brain Res*. 2008;190:53-69.
203. Gushue DL, Houck J, Lerner AL. Rabbit knee joint biomechanics: motion analysis and modeling of forces during hopping. *J Orthop Res*. 2005;23:735-742.
204. Martin RB, Chapman MW, Sharkey NA, et al. Bone ingrowth and mechanical properties of coralline hydroxyapatite 1 yr after implantation. *Biomaterials*. 1993;14:341-348.
205. Fenger JM, London CA, Kisseberth WC. Canine osteosarcoma: a naturally occurring disease to inform pediatric oncology. *ILAR J*. 2014;55:69-85.
206. Saulsman B, Oxnard CE, Franklin D. Long bone morphometrics for human from non-human discrimination. *Forensic Sci Int*. 2010;202(110):e111-115.
207. Landis WJ, Glimcher MJ. Electron diffraction and electron probe microanalysis of the mineral phase of bone tissue prepared by anhydrous techniques. *J Ultrastruct Res*. 1978;63:188-223.
208. Carrera EF, Nicolao FA, Netto NA, et al. A mechanical comparison between conventional and modified angular plates for proximal humeral fractures. *J Shoulder Elbow Surg*. 2008;17:631-636.
209. Lind PM, Lind L, Larsson S, et al. Torsional testing and peripheral quantitative computed tomography in rat humerus. *Bone*. 2001;29:265-270.
210. Zura R, Xiong Z, Einhorn T, et al. Epidemiology of fracture non-union in 18 human bones. *JAMA Surg*. 2016;151:e162775.
211. Tzioupis C, Giannoudis PV. Prevalence of long-bone non-unions. *Injury*. 2007;38:S3-S9.
212. Ekegren CL, Edwards ER, Steiger R, et al. Incidence, costs, and predictors of non-union, delayed union and Mal-union following long bone fracture. *Int J Environ Res Public Health*. 2018;15:2845. de .

213. Netto CC, Vieira VC, Marinheiro LP, et al. Are skeletally mature female rats a suitable model to study osteoporosis? *Arq Bras Endocrinol Metabol.* 2012;56:259-264.
214. Meinig RP, Buesing CM, Helm J, et al. Regeneration of diaphyseal bone defects using resorbable poly(L/DL-lactide) and poly(D-lactide) membranes in the Yucatan pig model. *J Orthop Trauma.* 1997;11:551-558.
215. Roschger P, Fratzl P, Eschberger J, et al. Validation of quantitative backscattered electron imaging for the measurement of mineral density distribution in human bone biopsies. *Bone.* 1998;23:319-326.
216. Garcia P, Histing T, Holstein JH, et al. Rodent animal models of delayed bone healing and non-union formation: a comprehensive review. *Eur Cell Mater.* 2013;26:1-12.
217. Bloebaum RD, Ota DT, Skedros JG, et al. Comparison of human and canine external femoral morphologies in the context of total hip replacement. *J Biomed Mater Res.* 1993;27:1149-1159.
218. Sumner DR Jr., Devlin TC, Winkelman D, et al. The geometry of the adult canine proximal femur. *J Orthop Res.* 1990;8:671-677.
219. Claes LE, Cunningham JL. Monitoring the mechanical properties of healing bone. *Clin Orthop Relat Res.* 2009;467:1964-1971.
220. Taguchi T, Koh R, Takawira C, et al. Agmatine for pain management in dogs with coxofemoral joint osteoarthritis: a pilot study. *Front Vet Sci.* 2018;5:311.
221. Lopez MJ, Quinn MM, Markel MD. Evaluation of gait kinetics in puppies with coxofemoral joint laxity. *Am J Vet Res.* 2006;67:236-241.
222. Seebeck P, Thompson MS, Parwani A, et al. Gait evaluation: a tool to monitor bone healing? *Clin Biomech.* 2005;20:883-891.
223. Kironde E, Sekimpi P, Kajja I, et al. Prevalence and patterns of traumatic bone loss following open long bone fractures at Mulago Hospital. *OTA Intl.* 2019;2:e015.
224. Fourie PD, Kirton AH, Jury KE. Growth and development of sheep: 2. Effect of breed and sex on growth and carcass composition of southdown and Romney and their cross. *New Zealand J Agric Res.* 1970;13:753.
225. Gautier E, Perren SM, Cordey J. Strain distribution in plated and unplated sheep tibia in an in vivo experiment. *Injury.* 2000;31(suppl 3):C37-44.
226. Herring SW, Mucci RJ. In vivo strain in cranial sutures: the zygomatic arch. *J Morphol.* 1991;207:225-239.
227. Herring SW, Rafferty KL, Liu ZJ, et al. Jaw muscles and the skull in mammals: the biomechanics of mastication. *Comp Biochem Physiol A Mol Integr Physiol.* 2001;131:207-219.
228. Renaud M, Farkasdi S, Pons C, et al. A new rat model for translational research in bone regeneration. *Tissue Eng Part C Methods.* 2016;22:125-131.
229. Vanecek V, Klima K, Kohout A, et al. The combination of mesenchymal stem cells and a bone scaffold in the treatment of vertebral body defects. *Eur Spine J.* 2013;22:2777-2786.
230. Sakata M, Tonomura H, Itsuji T, et al. Bone regeneration of osteoporotic vertebral body defects using platelet-rich plasma and gelatin beta-tricalcium phosphate sponges. *Tissue Eng Part A.* 2018;24:1001-1010.
231. Gunnella F, Kunisch E, Maenz S, et al. The GDF5 mutant BB-1 enhances the bone formation induced by an injectable, poly(l-lactide-co-glycolide) acid (PLGA) fiber-reinforced, brushite-forming cement in a sheep defect model of lumbar osteopenia. *Spine J.* 2018;18:357-369.
232. Eschler A, Roepenack P, Roesner J, et al. Cementless titanium mesh fixation of osteoporotic burst fractures of the lumbar spine leads to bony healing: results of an experimental sheep model. *Biomed Res Int.* 2016;2016:4094161.
233. Eschler A, Ropenack P, Herlyn PK, et al. The standardized creation of a lumbar spine vertebral compression fracture in a sheep osteoporosis model induced by ovariectomy, corticosteroid therapy and calcium/phosphorus/vitamin D-deficient diet. *Injury.* 2015;46(suppl 4):S17-23.
234. McLain RF, Yerby SA, Moseley TA. Comparative morphometry of L4 vertebrae: comparison of large animal models for the human lumbar spine. *Spine.* 2002;27:E200-206.
235. Busscher I, Ploegmakers JJ, Verkerke GJ, et al. Comparative anatomical dimensions of the complete human and porcine spine. *Eur Spine J.* 2010;19:1104-1114.
236. Denyer S, Bhimani AD, Papastefan S, et al. Magnetic kyphoplasty: A novel drug delivery system for the spinal column. *PLOS One.* 2018;13:e0201402.
237. Ando K, Imagama S, Kobayashi K, et al. Feasibility and effects of a self-assembling peptide as a scaffold in bone healing: an in vivo study in rabbit lumbar posterolateral fusion and tibial intramedullary models. *J Orthop Res.* 2018;36:3285-3293.
238. Glazer PA, Spencer UM, Alkalay RN, et al. In vivo evaluation of calcium sulfate as a bone graft substitute for lumbar spinal fusion. *Spine J.* 2001;1:395-401.
239. Kai T, Shao-qing G, Geng-ting D. In vivo evaluation of bone marrow stromal-derived osteoblasts-porous calcium phosphate ceramic composites as bone graft substitute for lumbar intervertebral spinal fusion. *Spine.* 2003;28:1653-1658.
240. Lopez MJ, McIntosh KR, Spencer ND, et al. Acceleration of spinal fusion using syngeneic and allogeneic adult adipose derived stem cells in a rat model. *J Orthop Res.* 2009;27:366-373.
241. Hwang K, You SH. Analysis of facial bone fractures: an 11-year study of 2094 patients. *Indian J Plast Surg.* 2010;43:42-48.
242. Eppley BL, Aalst JA, Robey A, et al. The spectrum of orofacial clefting. *Plast Reconstr Surg.* 2005;115:101e-114e.
243. Weijs WA. Mandibular movements of the albino rat during feeding. *J Morphol.* 1975;145:107-124.
244. Lieberman DE, Crompton AW. Why fuse the mandibular symphysis? A comparative analysis. *Am J Phys Anthropol.* 2000;112:517-540.
245. Alsagheer A, Kline LW, Doschak MR, et al. A novel experimental model for studying transverse orthodontic tooth movement in the rat mandible. *Angle Orthod.* 2013;83:774-781.
246. Kimura S, Kitagawa T. Some asymmetries in the weight, area and linear dimensions of the mandible of rats. *J Nihon Univ Sch Dent.* 1977;19:151-158.
247. Khojasteh A, Hosseinpour S, Dehghan MM, et al. Antibody-mediated osseous regeneration for bone tissue engineering in canine segmental defects. *Biomed Res Int.* 2018;2018:9508721.
248. Hussein KA, Zakhary IE, Elawady AR, et al. Difference in soft tissue response between immediate and delayed delivery suggests a new mechanism for recombinant human bone morphogenetic protein 2 action in large segmental bone defects. *Tissue Eng Part A.* 2012;18:665-675.
249. De Kok IJ, Peter SJ, Archambault M, et al. Investigation of allogeneic mesenchymal stem cell-based alveolar bone formation: preliminary findings. *Clin Oral Implants Res.* 2003;14:481-489.
250. Abu-Serriah M, Kontaxis A, Ayoub A, et al. Mechanical evaluation of mandibular defects reconstructed using osteogenic protein-1 (rhOP-1) in a sheep model: a critical analysis. *Int J Oral Maxillofac Surg.* 2005;34:287-293.
251. Abu-Serriah MM, Ayoub AF, Odell E, et al. A minimally invasive novel design for a vascular-pedicled bone segment for experimental studies of reconstruction of mandibular defects. *Br J Oral Maxillofac Surg.* 2004;42:236-240.
252. Aoki A, Kawamoto T, Aoki K, et al. Amount of bone lengthening affects blood flow recovery and bone mineralization after distraction osteogenesis in a canine cleft palate model. *Cleft Palate Craniofac J.* 2010;47:303-313.
253. Wang Y, Shi B, Li Y, et al. Comparative study of maxillary growth and occlusal outcome after autogenous rib grafting in complete cleft palate defect. *J Craniofac Surg.* 2006;17:68-79.

254. Caballero M, Jones DC, Shan Z, et al. Tissue engineering strategies to improve osteogenesis in the juvenile swine alveolar cleft model. *Tissue Eng Part C Methods*. 2017;23:889-899.
255. Sato A, Yanagi T, Yamaguchi Y, et al. Effect of DNA/protamine complex paste on bone augmentation of the mandible: a pilot study on dogs. *Arch Oral Biol*. 2020;115:104729.

How to cite this article: Taguchi T, Lopez MJ. An overview of de novo bone generation in animal models. *J Orthop Res*. 2021;39:7–21. <https://doi.org/10.1002/jor.24852>